Osteoclast-Mediated Bone Resorption is Controlled by a Compensatory Network of Secreted and Membrane-Tethered Metalloproteinases

Lingxin Zhu,[1,2,3]* Yi Tang,[2,3] Xiao-Yan Li,[2,3] Evan T. Keller,[5] Jingwen Yang,[1,4] Jung-Sun Cho,[2,3] Tamar Y. Feinberg,[2,3] and Stephen J. Weiss[2,3]*

SUPPLEMENTARY MATERIALS

Materials and methods

RNA extraction and gene expression analysis

RNA was isolated from cultured cells with TRIzol reagent (Invitrogen) and purified using QIAGEN RNeasy Mini-kit columns (QIAGEN). RNA quality was confirmed using an Agilent 2100 Bioanalyzer and samples profiled on Mouse Gene 2.1 ST expression arrays (Affymetrix). Each sample was analyzed at the University of Michigan Microarray Core as previously described (*22, 34*). Expression values for each probe set were calculated using a robust multi-array average (RMA) (*84*). Microarray data are available at Gene Expression Omnibus (GEO) under accession numbers: GSE138324. Mouse complementary DNA (cDNA) was reverse-transcribed from 1 μg total RNA with SuperScript VILO Master Mix (Life Technologies). qPCR was performed in triplicate samples using SYBR Green PCR master mix (Applied Biosystems) according to the manufacturer's instructions. For each transcript examined, mRNA levels were normalized to *Gapdh/GAPDH* levels. The primers used were constructed as described in the Supplemental Material. For quantitative real-time PCR primers, see Table S2.

Western blot analysis

Cell lysate preparation and sodium dodecyl sulfate-polyacrylamide gel electrophoresis (SDS-PAGE) and Western blotting carried out according to standard protocol. Proteins were harvested in cell lysis buffer supplemented with proteinase inhibitor cocktail (Sigma-Aldrich) and phosphatase inhibitor cocktail 2 (Sigma-Aldrich). Antigen detection was performed using antibodies directed against Mmp9 (Abcam), Mmp14 (Abcam), NFATc1 (Santa Cruz), c-Fos (Cell Signaling), c-Src (Cell Signaling), Ctsk (Santa Cruz), type I collagen (Sigma-Aldrich), α-tubulin (Abcam), GAPDH (Cell Signaling), or β-actin (Cell Signaling). Bound primary antibodies were detected with horseradish peroxidase-conjugated species-specific secondary antibodies (Santa Cruz) using the Super Signal Pico system (Thermofisher Scientific). Full images of Western blots are presented in fig. S8.

Immunofluorescent staining

For immunofluorescent staining, osteoclasts were fixed with 4% paraformaldehyde, permeabilized with 0.1% Triton X-100, blocked for 1h prior to an overnight incubation at 4°C with primary antibodies directed against Mmp9 (Abcam, ab38898; 1:300) or β-gal (Abcam, ab9361; 1:400). For bone tissue immunofluorescent staining, femurs from 10-wk old *Mmp14*$^{+/LacZ}$ mice were fixed in 4% paraformaldehyde at 4°C overnight, decalcified in 10% EDTA and transferred to 30% sucrose in PBS for embedding in OCT (Fisher Healthcare). Frozen sections were permeabilized with 0.3-0.5% Triton X-100 in PBS, and blocked for 2 h prior to adding primary antibodies directed against Mmp9 (Abcam, ab38898; 1:300) or β-gal (Abcam, ab9361; 1:10,000). Following primary antibody incubations, sections were incubated with Alexa 488- or Alexa 594-conjugated secondary antibodies (Invitrogen Molecular Probes). Nuclei were visualized by staining with 1 μg/ml 4′,6-diamidino-2-phenylindole (DAPI). For F-actin staining, osteoclasts were incubated with FITC- or Alexa Fluor 647-conjugated phalloidin (Sigma-Aldrich). Fluorescence images were acquired with an Olympus FluoView FV500 laser-scanning confocal microscope and analyzed with Adobe Photoshop and Image J software.

Flow cytometry analysis

Single-cell suspensions of osteoclast precursor cells were collected after passing through a 40 μm cell strainer (BD Bioscience), incubated with Fc block (eBioscience) for 10 min, and then incubated with Alexa Fluor 488-conjugated anti-CD11b (M1/70; eBioscience) or the corresponding isotype control (eBioscience) in flow cytometry staining buffer (eBioscience) for 25 min at 4 °C prior to analysis on a FACS Canto II (BD Bioscience).

Cell proliferation assay

Cells were seeded at 1×10^4 cells per well in 96-well plates and proliferation determined using the cell proliferation reagent, WST-1 (Sigma-Aldrich), according to the manufacturer's instructions.

Osteoclast acid production

Acid production was determined using acridine orange as described *(85)*. To assess intracellular pH, osteoclasts differentiated on cortical bone slices were incubated in MEM buffered at pH 7.4 with 20 mM HEPES and containing 5 μg/ml acridine orange (Invitrogen) for 15 min at 37°C, washed, and imaged using

a confocal microscope (excitation, 488 nm; emission, 500–550 nm [green form] and 570–620 nm [red/orange acidic form]).

Collagenolysis of decalcified bone slices

COS-1 cells were transiently transfected with cDNAs encoding full-length human MMP9 or a soluble human MMP14 construct (Met^{1}-Gly^{535}) that lacks the COOH-terminal transmembrane and cytosolic domains of the wild-type proteinase) in pCR3.1 vectors (*86*), using Fugene (Roche) according to the manufacturer's instructions. The cells were then incubated in serum-free DMEM for 24 h to collect MMP9 or soluble MMP14-conditioned medium. Proteinase concentrations in the conditioned media were titrated with TIMP2 (*87*), and calculated using a matrix metalloproteinase activity assay kit (Abcam).

Cortical bovine bone slices were decalcified in 10% EDTA for 2 weeks, with fresh EDTA solutions changed every 2 d. Decalcification was verified by von Kossa staining and compared with normal calcified bone slices prior to use. The decalcified bone slices were incubated with MMP9-conditioned media (~10 μg active MMP9) activated with 1 mM 4-aminophenyl mercuric acetate (APMA), or soluble MMP14-conditioned medium (~8 μg active MMP14) at 37°C for 24 h in the presence or absence of 5 μM BB-94 (Tocris Bioscience) in 50 mM Tris-HCl (pH 7.5) supplemented with 10 mM $CaCl_2$, 150 mM NaCl, 5 μM $ZnCl_2$ and 0.05% Brij-35 (w/v). A hydroxyproline colorimetric assay kit (BioVision) was used to quantify the collagen degradation products released into the conditioned medium as described (*46*).

Bone surface biotin labeling

Bone surface was labeled with biotin as described (*88*). Briefly, cortical bone slices were incubated in PBS containing 2 mg/ml sulfo-N-hydroxysuccinimide-biotin (Thermofisher Scientific) for 2 h, washed repeatedly, and rinsed overnight in PBS. Osteoclasts were then cultured on biotin-labeled bone slices. After fixation, biotinylated bone materials inside osteoclasts were visualized with FITC-conjugated streptavidin (Thermofisher Scientific) for 2 h at room temperature.

Scanning electron microscope (SEM) analysis

Cultured bone following osteoclasts removal or decalcified bone slices were fixed overnight in 2.5% glutaraldehyde in 0.1 M Sorensen's phosphate buffer (pH 7.4). Samples were then dehydrated in ascending ethanol series, processed for critical point drying (Balzers Union, Balzers, Lichtenstein) and Au/Pg

sputtered (E-5100, Polaron Equipment Ltd., East Grinstead, UK). Samples were imaged on an AMRAY 1910 field emission scanning electron microscope.

Whole bone mechanical four-point bending

Destructive four-point bending tests were performed on explanted femurs using a servohydraulic testing device (MTS 858 MiniBionix, Eden Prairie, MN) as described *(89)*. The femurs were loaded on support bars with the posterior surface oriented under tension. The distance between the wide, upper support bars was 6.26 mm, and the span between the narrow, lower support bars was 2.085 mm. The vertical displacement rate of the four-point bending apparatus in the anterior–posterior direction was 0.5 mm/s. Force was recorded by a 50 lb load cell (Sensotec) and vertical displacement by an external linear variable differential transducer (LVDT, Lucas Schavitts, Hampton, VA), both at 2000 Hz. A custom MATLAB script was used to analyze the raw force displacement data and calculate all four-point bending parameters.

Fig. S1

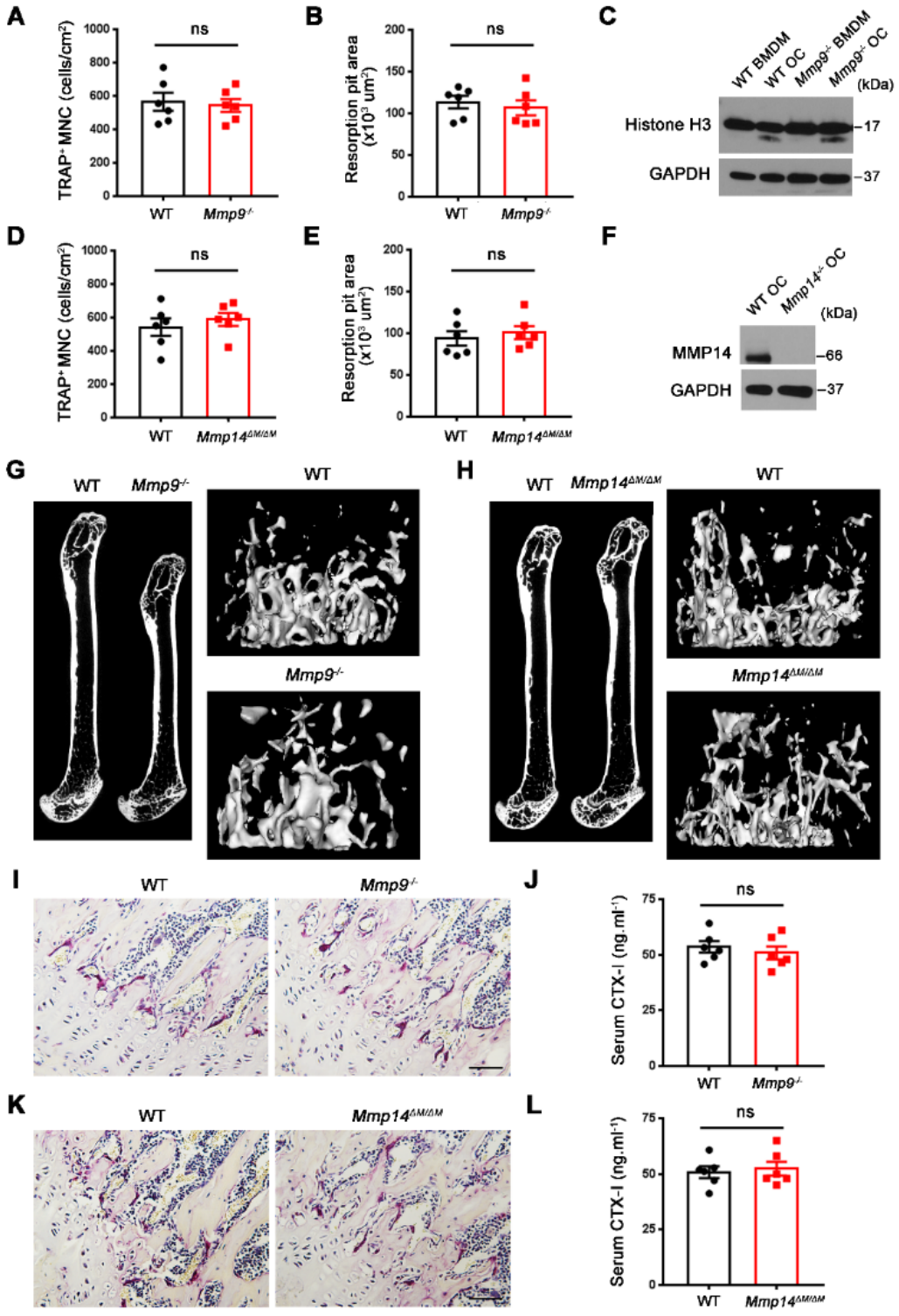

Fig. S1. *Mmp9*$^{-/-}$ and myeloid-specific *Mmp14* conditional knockout mice exhibit normal osteoclast activity *in vitro* and *in vivo*. (A) BMDMs were isolated from wild-type or *Mmp9*$^{-/-}$ mice and cultured on

plastic substrata with M-CSF and RANKL for 5 d, and the number of $TRAP^+$ MNCs determined (n = 6). (B) Wild-type or *Mmp9*$^{-/-}$ BMDMs were cultured atop bone slices and induced into osteoclasts for 6 days, osteoclasts were then removed, resorption pits visualized by WGA-DAB staining and resorption pit area quantified (n = 6). (C) Western blot of Histone H3 in BMDMs and osteoclasts generated from wild-type or *Mmp9*$^{-/-}$ mice. (D) BMDMs were isolated from wild-type or *Mmp14*$^{\Delta M/\Delta M}$ mice and cultured on plastic substrata with M-CSF and RANKL for 5 d, and $TRAP^+$ MNCs quantified (n = 6). (E) Wild-type or *Mmp14*$^{\Delta M/\Delta M}$ BMDMs were cultured atop bone slices and induced into osteoclasts for 6 days, osteoclasts were then removed, resorption pits visualized by WGA-DAB staining and resorption pit area quantified (n = 6). (F) Western blot of Mmp14 in osteoclasts generated from wild-type or *Mmp14*$^{\Delta M/\Delta M}$ mice. (G, H) Representative microcomputed tomography of sagittal sections of femurs with 3D reconstruction of distal femur trabeculae near the growth plate in 5 month-old (G) wild-type and *Mmp9*$^{-/-}$ male mice or (H) wild-type and *Mmp14*$^{\Delta M/\Delta M}$ male mice. (I) TRAP-staining of distal femurs in 5 month-old wild-type and *Mmp9*$^{-/-}$ male mice. Scale bar, 100 μm. (J) Serum CTX-I levels in 5 month-old wild-type and *Mmp9*$^{-/-}$ male mice. (K) TRAP-staining of distal femur in 5 month-old wild-type and *Mmp14*$^{\Delta M/\Delta M}$ male mice. Scale bar, 100 μm. (L) Serum CTX-I levels in 5 month-old wild-type and *Mmp14*$^{\Delta M/\Delta M}$ male mice. All results are representative of data generated from at least 3 independent experiments. ns, not significant. Error bars are mean ± SEM. All data were analyzed using unpaired Student's t test.

Fig. S2

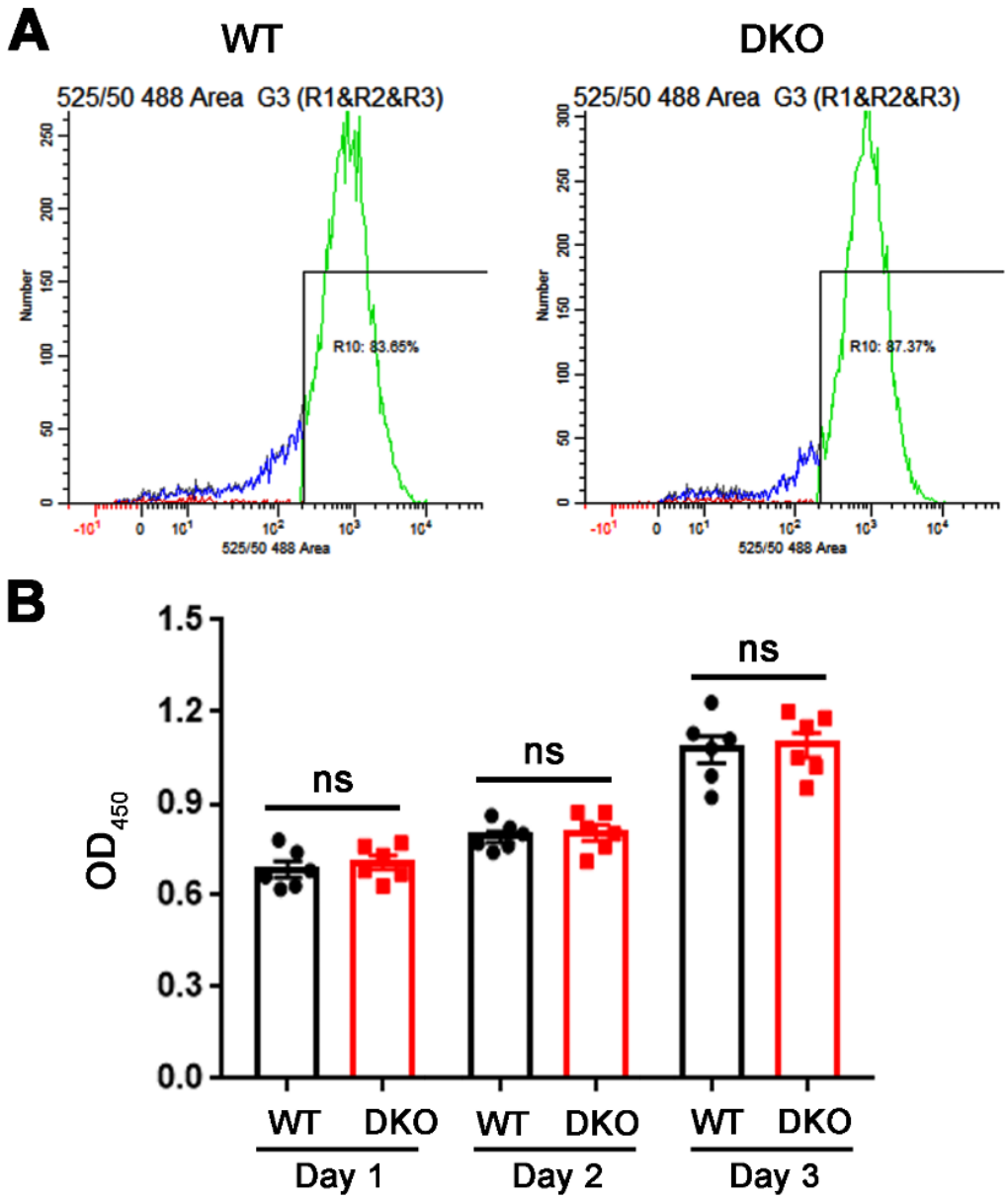

Fig. S2. Characterization of *Mmp9/Mmp14* DKO osteoclast precursors. (A) CD11b expression levels in wild-type or DKO osteoclast precursor cells as determined by flow cytometry. (B) Proliferation of wild-type and DKO BMDMs by WST-1 assay ($n = 6$). All results are representative of data generated in at least three independent experiments. ns, not significant. Error bars are mean ± SEM. Data were analyzed using unpaired Student's *t* test.

Fig. S3

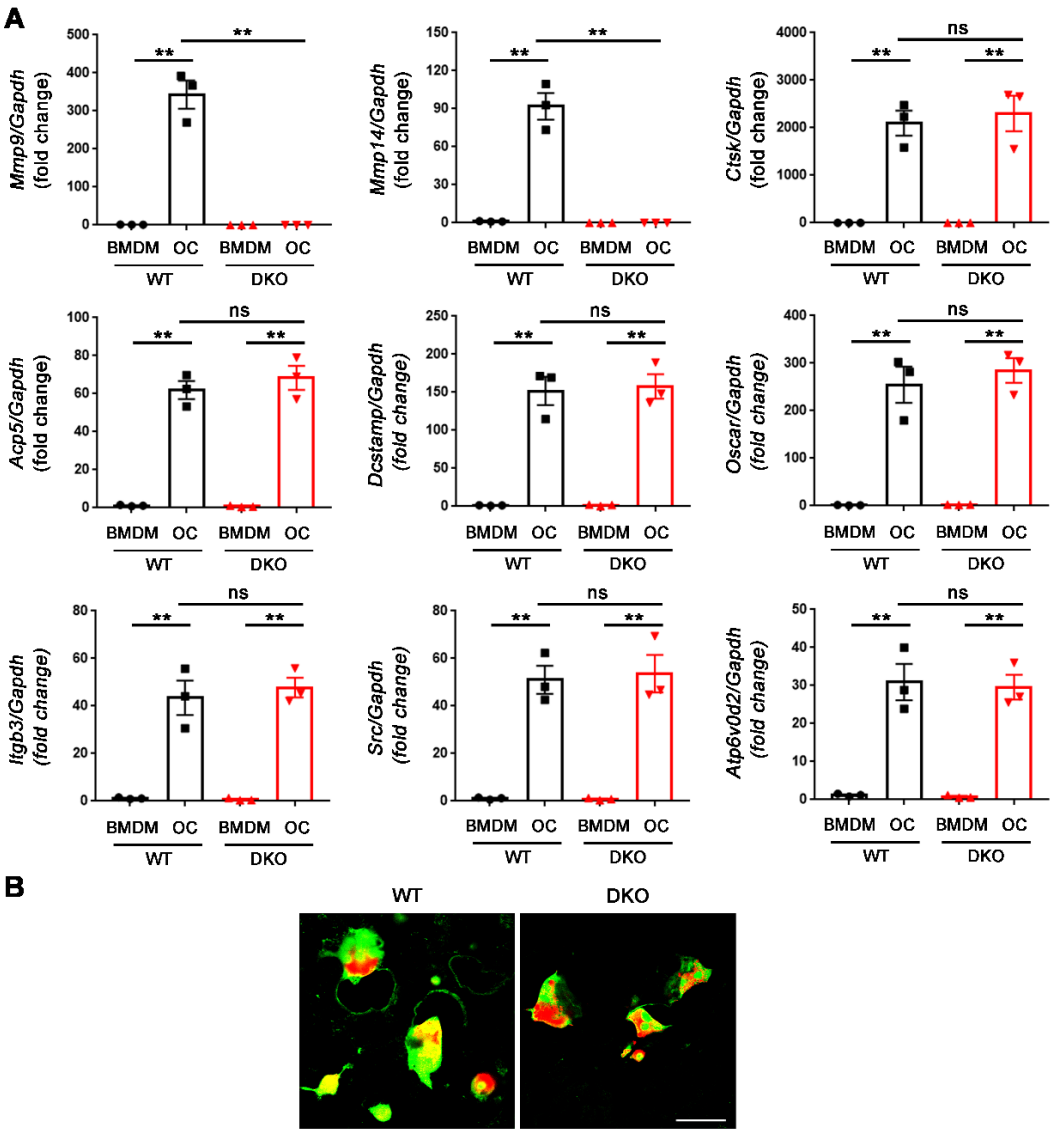

Fig. S3. *Mmp9/Mmp14* DKO osteoclasts display normal osteoclastogenesis, gene expression and intracellular acidification. (A) Relative mRNA expression of *Mmp9, Mmp14, Ctsk*, *Acp5*, *Dcstamp*, *Oscar*, *Itgb3*, *Src* and *Atp6v0d2* in BMDMs and osteoclasts generated from wild-type or DKO mice (n = 3). (B) BMDMs were isolated from wild-type or DKO mice and cultured atop bone slices with M-CSF and RANKL for 6 d. Acidification of osteoclast lacunar zones was visualized by acridine orange staining. Scale bar, 50 μm. All results are representative of data generated in at least three independent experiments. ns, not significant; $^{**}P < 0.01$. Error bars are mean ± SEM. All data were analyzed using two-way ANOVA with Bonferroni correction.

Fig. S4

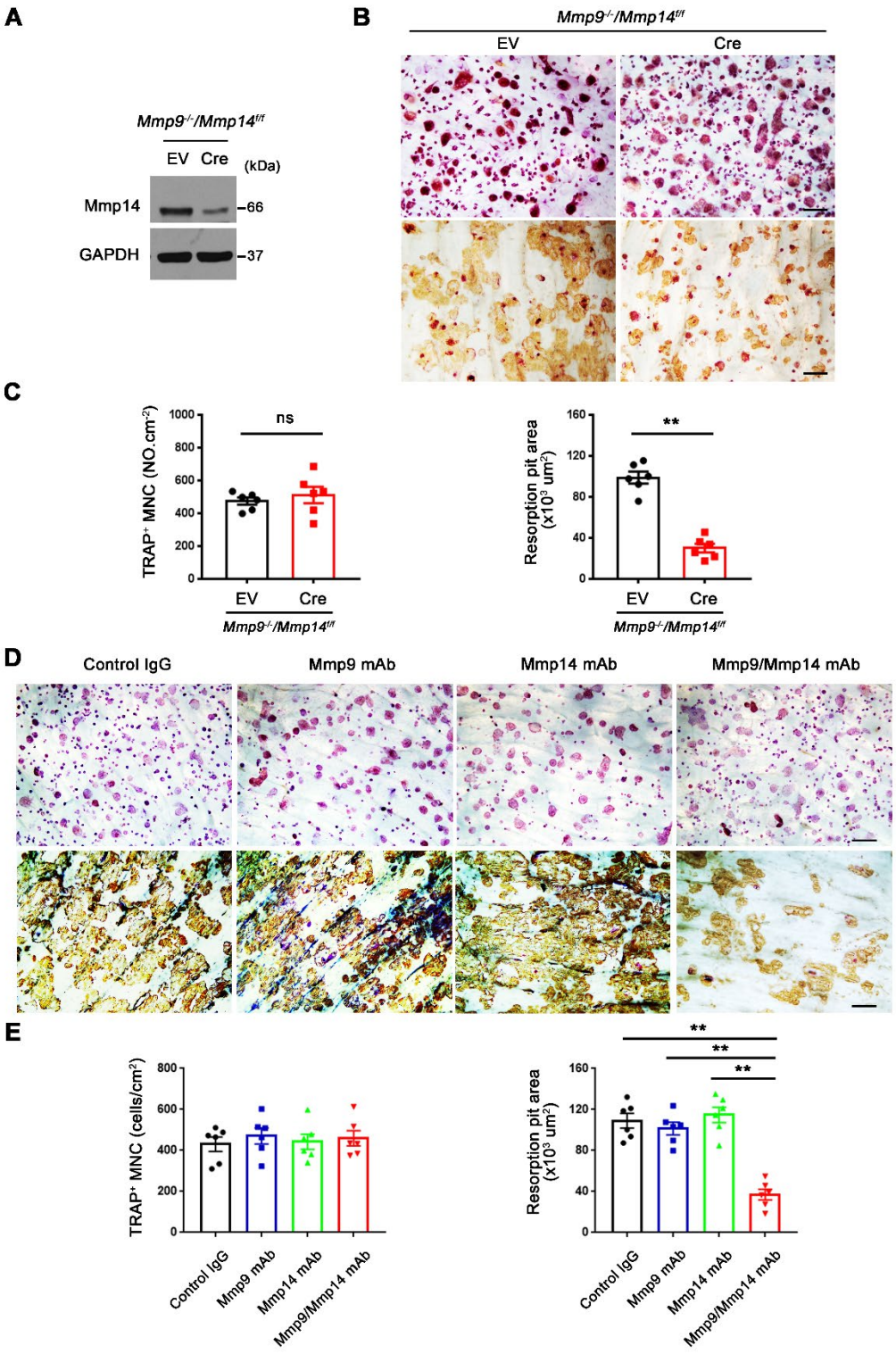

Fig. S4. Temporal requirements for Mmp9 and Mmp14 in supporting osteoclast function. (A) *Mmp9*$^{-/-}$*/Mmp14*$^{f/f}$ BMDMs were transduced with a lentiviral Cre or an empty expression vector (EV),

differentiated into osteoclasts, and cell lysates collected for Mmp14 immunoblotting. (B) Lentiviral Cre or empty expression vector-transduced *Mmp9*$^{-/-}$*/Mmp14*$^{f/f}$ BMDMs were induced into osteoclasts, cultured atop bone slices for 6 days and cells stained for TRAP activity. Following osteoclast removal, resorption pits were visualized by WGA-DAB staining. Scale bar, 100 μm. (C) Quantification of TRAP and WGA staining described in B ($n = 6$). ns, not significant; $^{**}P < 0.01$. (D) Mouse osteoclasts were cultured atop bone slices in the presence or absence of 100 μg/ml of either the Mmp9 or Mmp14 blocking antibodies, or an IgG control for 3 days. Osteoclasts were then stained for TRAP activity. Following osteoclast removal, resorption pits were visualized by WGA-DAB staining. Scale bar, 100 μm. (E) Quantification of TRAP and WGA staining in D ($n = 6$). All results are representative of data generated in at least three independent experiments. ns, not significant; $^{**}P < 0.01$. Error bars are mean ± SEM. Data were analyzed using unpaired Student's *t* test (C) or one-way ANOVA with Bonferroni correction (E).

Fig. S5

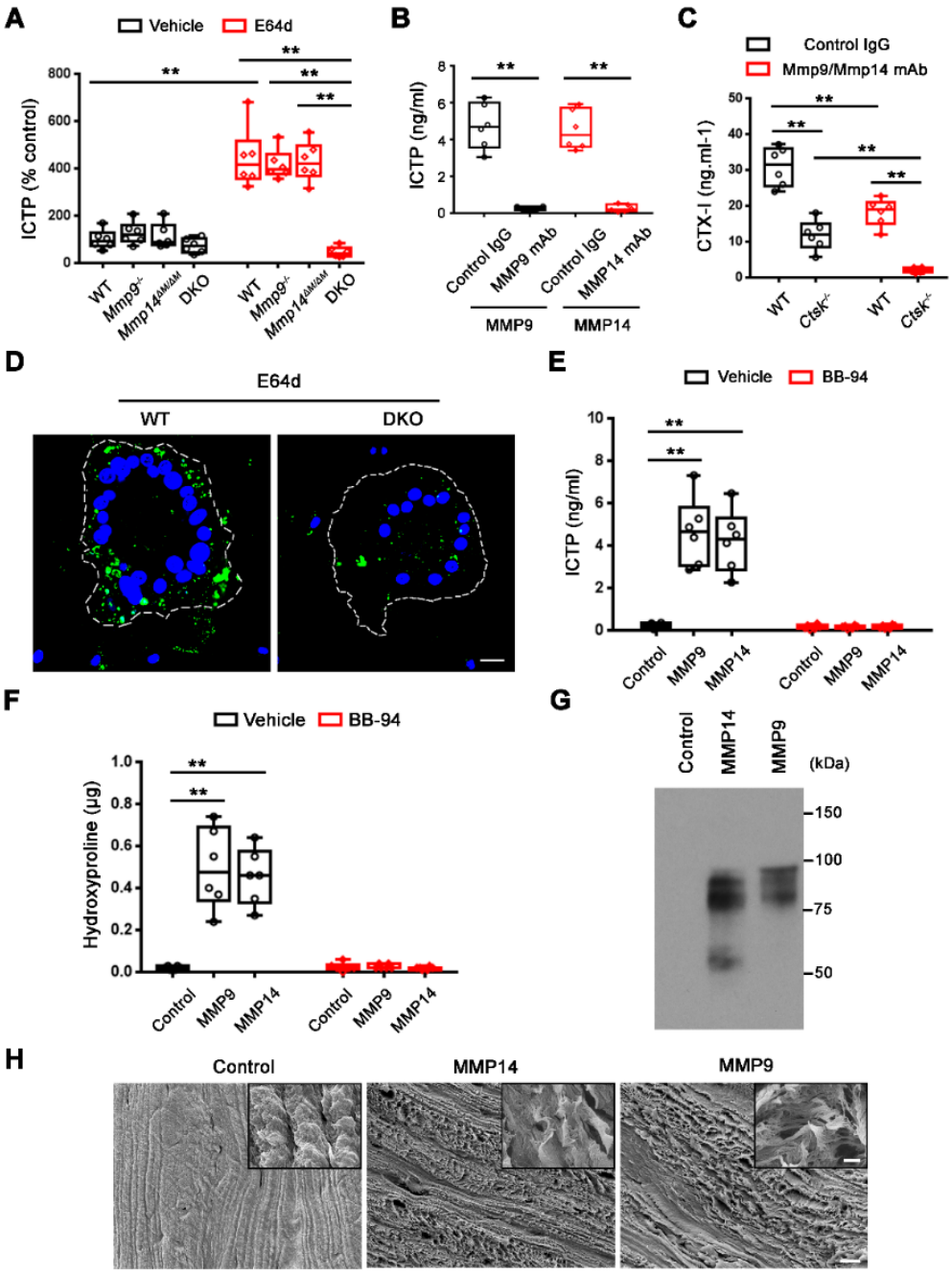

Fig. S5. Osteoclast Mmp9/Mmp14 activities co-determine bone type I collagenolysis. (A) Osteoclasts differentiated from wild-type, *Mmp9*$^{-/-}$, *Mmp14*$^{\Delta M/\Delta M}$ or DKO BMDMs were cultured atop native cortical bone slices with or without 20 µM E64d for 6 days, and supernatants collected for ICTP ELISA (n = 6). (B) Active MMP9 or active, soluble MMP14 was incubated with decalcified cortical bone slices for 24 h in the absence or presence of control or neutralizing monoclonal antibodies directed against MMP9 or

MMP14 and ICTP levels determined ($n = 4$). (C) Wild-type or *Ctsk*$^{-/-}$ osteoclasts were cultured atop cortical bone slices in the presence or absence of the Mmp9 and Mmp14 blocking antibodies, and supernatants collected for CTX-I ELISA ($n = 6$). (D) Osteoclasts differentiated from wild-type or DKO BMDMs were cultured atop biotin-labeled cortical bone slices with 20 μM E64d for 6 days. Then biotinylated bone material inside cells was visualized with FITC-conjugated streptavidin. (E, F) Active MMP9 or active, soluble MMP14 was incubated with decalcified cortical bone slices for 24 h in the absence or presence of 5 μM BB-94 or a DMSO control and either ICTP (E) or hydroxyproline (F) levels determined ($n = 6$). (G, H) Supernatants recovered from decalcified cortical bone slices after incubation with active MMP9 or active, soluble MMP14 were collected for type I collagen immunoblotting (G), and the decalcified bone slices were imaged by SEM (H). Scale bar, 10 μm; inset scale bar, 1 μm. All results are representative of data generated in at least three independent experiments. $^{**}P < 0.01$. Error bars are mean ± SEM. All data were analyzed using two-way ANOVA with Bonferroni correction.

Fig. S6

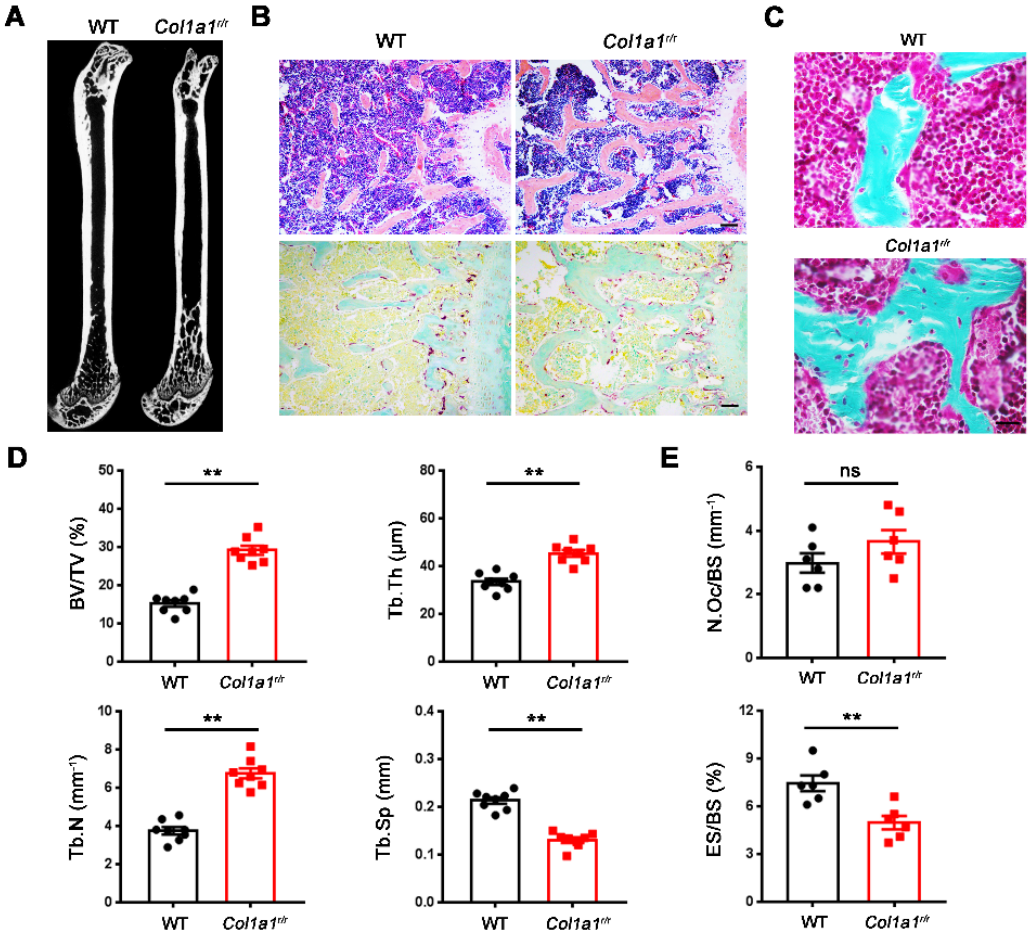

Fig. S6. *Col1a*$^{r/r}$ mutant mice exhibit an osteopetrotic phenotype *in vivo*. (A) Representative microcomputed tomography of sagittal sections of femurs from 5 month-old wild-type and *Col1a*$^{r/r}$ male mice. (B) H&E and TRAP staining of distal femurs in 5 month-old wild-type and *Col1a*$^{r/r}$ male mice. Scale bar, 100 μm. (C) Golden's trichrome staining of distal femur in 5 month-old wild-type and *Col1a*$^{r/r}$ male mice. Scale bar, 20 μm. (D) Quantification of bone volume/tissue volume (BV/TV), trabecular thickness (Tb.Th), trabecular number (Tb.N), and trabecular separation (Tb.Sp) as measured by microcomputed tomography in 5 month-old wild-type and *Col1a*$^{r/r}$ male mice (n = 8). (E) Quantification of osteoclast number per bone surface (N.Oc/BS) and eroded surface per bone surface (ES/BS) in 5 month-old wild-type and *Col1a*$^{r/r}$ male mice (n = 6). All results are representative of data generated in at least 3 independent experiments. ns, not significant; **$P < 0.01$. All data were analyzed using unpaired Student's t test.

Fig. S7

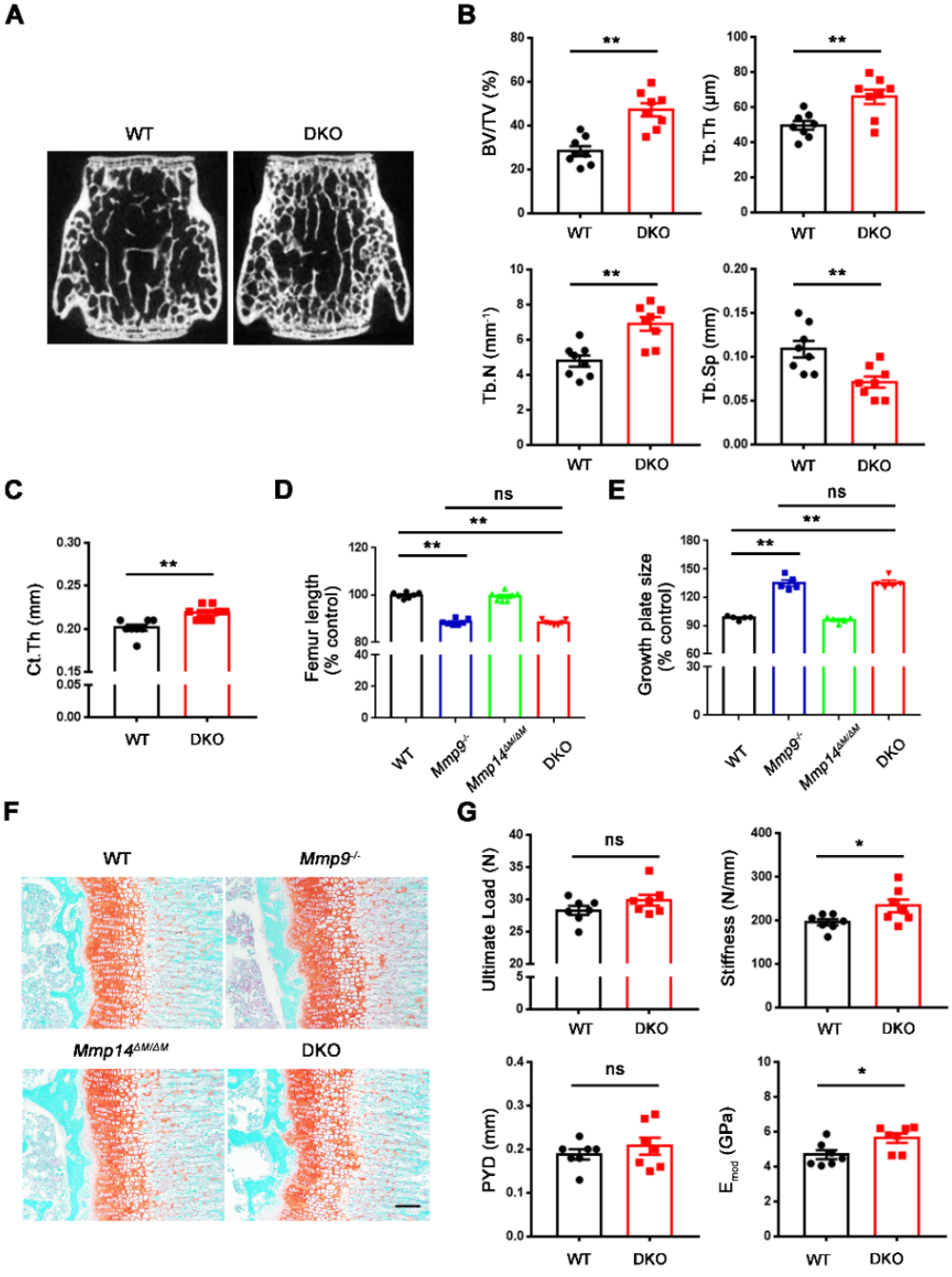

Fig. S7. *Mmp9/Mmp14* DKO mice exhibit increased bone mass in lumbar vertebrae and display improved biomechanical properties. (A) Representative microcomputed tomography of L3 vertebrae sections of 5 month-old wild-type and DKO male mice are shown. (B) Quantification of bone volume/tissue volume (BV/TV), trabecular thickness (Tb.Th), trabecular number (Tb.N), and trabecular separation

(Tb.Sp) as determined by microcomputed tomography in L3 vertebrae of 5 month-old wild-type and DKO male mice (n = 8). (C) Quantification of cortical thickness (Ct.Th) as determined by microcomputed tomography in femurs of 5 month-old wild-type and DKO male mice (n = 8). (D) Quantification of femur length as determined by microcomputed tomography in femurs of 5 month-old wild-type, *Mmp9*$^{-/-}$, *Mmp14*$^{\Delta M/\Delta M}$, and DKO male mice (n = 7). (E) Quantification of growth plate size as determined by Safarin O and fast green staining in femurs of 1 month-old male wild-type, *Mmp9*$^{-/-}$, *Mmp14*$^{\Delta M/\Delta M}$, and DKO male mice (n = 5). (F) Safarin O and fast green staining of the distal femurs of 1 month-old male wild-type, *Mmp9*$^{-/-}$, *Mmp14*$^{\Delta M/\Delta M}$, and DKO mice. Scale bar, 100 μm. (G) Ultimate load, stiffness, post-yield displacement (PYD), and elasticity modulus (E_{mod}) analyzed using four-point bending test (n = 7). ns, not significant; *P < 0.05; **P < 0.01. Error bars are mean ± SEM. Data were analyzed using unpaired Student's t test (B, C and G) or one-way ANOVA (D and E) with Bonferroni correction.

Fig. S8

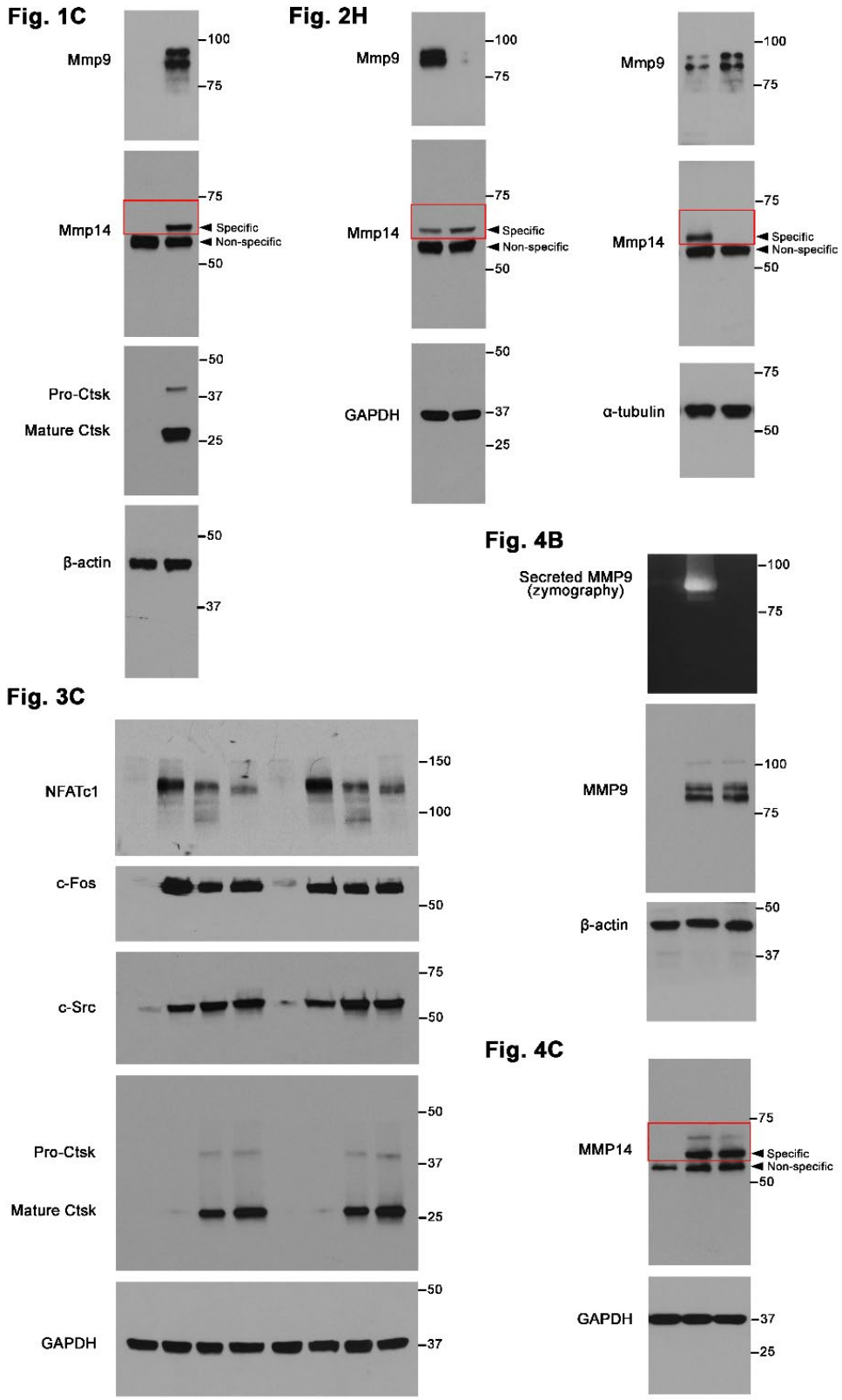
Fig. 1C
Mmp9
100
75
Mmp14
75
Specific
Non-specific
50
Pro-Ctsk
Mature Ctsk
50
37
25
β-actin
50
37
Fig. 2H
Mmp9
100
75
Mmp14
75
Specific
Non-specific
50
GAPDH
50
37
25
Mmp9
100
75
Mmp14
75
Specific
Non-specific
50
α-tubulin
75
50
Fig. 4B
Secreted MMP9
(zymography)
100
75
MMP9
100
75
β-actin
50
37
Fig. 3C
NFATc1
150
100
c-Fos
50
c-Src
75
50
Pro-Ctsk
Mature Ctsk
50
37
25
GAPDH
50
37
Fig. 4C
MMP14
75
Specific
Non-specific
50
GAPDH
37
25

Fig. S8 continued

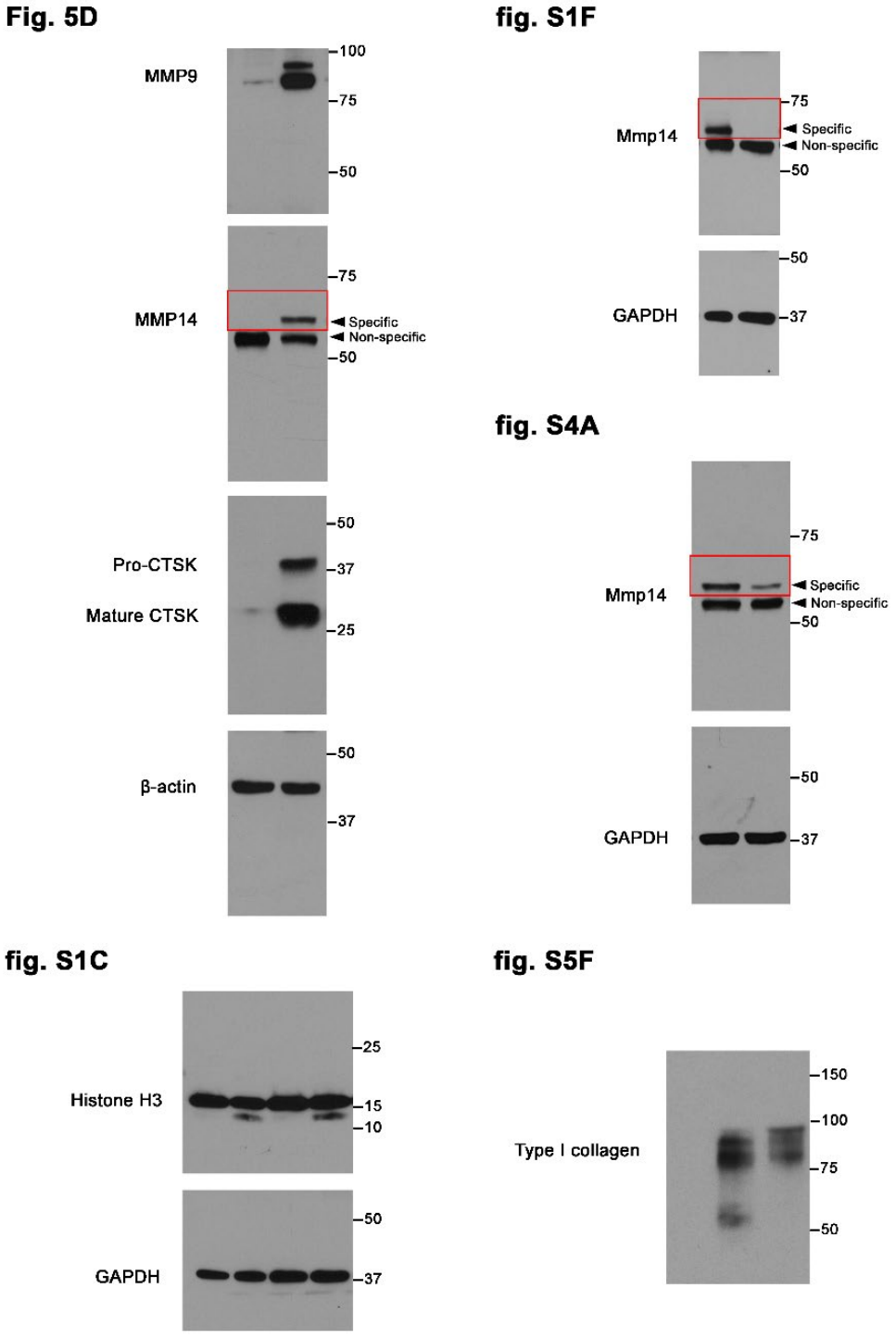

Fig. S8. Western blotting films. Uncropped images of scanned western blots shown in Figures and Supplementary Figures are provided.

Table S1. Genotyping PCR primers

Allele	Forward (5' to 3')	Reverse (5' to 3')
Mmp14^{lacZ}(+)	ACCTGCGTGCAATCCATCTTG	ATGATGGCGGAGGGATCGTTAG
Mmp14^{lacZ}(-)	TGAGGTGGAAAACACGACCAG	ATGATGGCGGAGGGATCGTTAG
Mmp9^{WT}	TCCCACTTGAGGCCTTTGA	TCCTCCATCCACAGGCATAC
Mmp9^{KO}	CCTTCTATCGCCTTCTTGACG	TCCTCCATCCACAGGCATAC
Mmp14^{flox}	GTTGAGGCAGGAGGATTGTGAGT T	CCTGGAAAAGTGGGCGAGAAG
Csf1r-Cre	ACAACTACCTGTTCTGCCG	GCCTCAAAGATCCCTTCCAG
Col1a1^{r}	TGGTTCTGGAATGAGGATGG	TGCCTCTGCTTCCTTAGTGC

Table S2. Quantitative real-time PCR primers

Gene	Forward (5' to 3')	Reverse (5' to 3')
Mouse Mmp9	CTGGACAGCCAGACACTAAAG	CTCGCGGCAAGTCTTCAGAG
Mouse Mmp14	CAGTATGGCTACCTACCTCCAG	GCCTTGCCTGTCACTTGTAAA
Mouse Ctsk	AGGTCGGTGTGAACGGATTTG	TGTAGACCATGTAGTTGAGGTCA
Mouse Acp5	CACTCCCACCCTGAGATTTGT	CCCCAGAGACATGATGAAGTCA
Mouse Dcstamp	GGGGACTTATGTGTTTCCACG	ACAAAGCAACAGACTCCCAAAT
Mouse Oscar	CCTAGCCTCATACCCCCAG	CGTTGATCCCAGGAGTCACAA
Mouse Itgb3	CCACACGAGGCGTGAACTC	CTTCAGGTTACATCGGGGTGA
Mouse Src	GAACCCGAGAGGGACCTTC	GAGGCAGTAGGCACCTTTTGT
Mouse Atp6v0d2	CAGAGCTGTACTTCAATGTGGAC	AGGTCTCACACTGCACTAGGT
Mouse Gapdh	AGGTCGGTGTGAACGGATTTG	AGGTCGGTGTGAACGGATTTG
Human MMP9	TGTACCGCTATGGTTACACTCG	GGCAGGGACAGTTGCTTCT
Human MMP14	GGCTACAGCAATATGGCTACC	GATGGCCGCTGAGAGTGAC
Human CTSK	ACACCCACTGGGAGCTATG	GACAGGGGTACTTTGAGTCCA
Human GAPDH	GGAGCGAGATCCCTCCAAAAT	GGCTGTTGTCATACTTCTCATGG